A New Scintillator for Neutron Scattering Instruments

Dr. J. Bart Czirr
Mission Support Incorporated/Photogenics

We have developed an efficient new scintillator material that contains lithium, gadolinium and boron, all three of which possess large neutron capture cross sections for highly exothermic reactions. In addition, all three materials have low cross section isotopes that can be utilized to select the reactions of interest. The new material, Li_6 Gd $(BO_3)_3$ activated with trivalent cerium, can be grown as clear single crystals suitable for large area neutron detectors. The outstanding characteristic of these materials is the high scintillation efficiency—as much as six times that of Li-glass scintillators. This increase in light output permits the practical use of the exothermic ^{10}B (n, alpha) reaction for low energy neutron detection. This reaction provides a four-fold increase in capture cross section relative to the ^{6}Li (n, alpha) reaction plus the intriguing possibility of demanding a charged-particle/gamma-ray coincidence to reduce background rates. These new materials will be useful in the thermal and epithermal energy ranges at reactors and pulsed neutron sources.

Four exothermic neutron capture reactions dominate the low-energy neutron detector field: ^{3}He (n,p)T, ^{6}Li (n,$\propto$) T, ^{10}B (n,$\propto$) ^{7}Li, and Gd(n,gamma). The ^{3}He reaction utilized in gaseous proportional counters has been the most popular system for several decades, but Li based scintillators have begun to supplant these detectors at both reactors and pulsed sources. Aside from BF_3 proportional counters, no practical ^{10}B-based detectors have been available. This is unfortunate, because the ^{10}B (n,$\propto$) reaction possesses several advantages over the other reactions, namely:

The capture cross section of ^{10}B is 4.1 times that of ^{6}Li.

The maximum range of the ^{10}B charged reaction products is 4 microns vs 40 microns for ^{6}Li. This permits the use of thinner detectors and could also result in superior spatial resolution in some situations.

The 478 keV gamma ray that is emitted in 94% of the capture reactions in ^{10}B can be utilized as a coincidence signal to greatly reduce the effects of ambient gamma background.

A condensed state ^{10}B detector will be much more efficient in thin layers that gaseous detectors.

Edge effects are greatly reduced in solid detectors.

In scintillator form, the ^{10}B detector recovery time can be much shorter than that of proportional counters.

The primary characteristic that has inhibited the use of ^{10}B-based scintillators is the low scintillation efficiency of B-loaded organic scintillators. The high energy-loss rate of the heavy charged reaction products is particularly detrimental to the efficient production of scintillation light in organic scintillator solvents. For example, in BC-454 plastic the light output per unit energy for the combined $\propto$, ^{7}Li signal from ^{10}B capture is only 4% that of electrons of the same energy. Another measure of the seriousness of this problem is that the light output for the ^{10}B reaction (2.31 MeV) is only 10% of that for the ^{6}Li reaction (4.79MeV), for liquid organic scintillators.

In light of the significant advantages attached to the ^{10}B reaction, it seemed useful to search for a B-based scintillator with greatly improved scintillation efficiency. The lithium lanthanide borates have been reported in the literature as a class of stoichiometric laser materials which can incorporate three of the popular neutron absorbing nuclei: B, Li and Gd(1). When activated with Ce^{3+}, these materials achieve a remarkably high scintillation efficiency compared to organic scintillators. Table I lists the measured signal size of Li_6Gd $(BO_3)_3$(Ce) compared to the three most efficient competing materials. In addition, the estimated absolute number of detected photoelectrons in a typical PM tube is shown for the three reactions of interest. These latter numbers are based upon a measured value of 1025 photoelectrons per captured neutron in GS-20 glass scintillator. The observed factor of six improvement (over GS-20) in scintillation efficiency compensates for the factor of five decrease in light output from ^{6}Li to ^{10}B in the borate scintillator. The result is that the signal size from the present sample of Li_6Gd $(BO_3)_3$(Ce) upon ^{10}B capture exceeds that of GS-20 for ^{6}Li capture. This result should provide a practical, good-pulse-height-resolution signal for many applications. Another material, with similar chemical and crystal-structure properties is $Li_6Y(BO_3)_3$(Ce). The

advantage in substituting Y for Gd arises from the much lower neutron capture cross section for naturally occurring Y, thereby removing the strong competition for neutrons below 150 meV.

For applications requiring large-area detectors, it is advisable to use the borate crystals in powdered form incorporated within a transparent binder. Fortunately, the index of refraction of the crystals is within the range of transparent organic polymers. In particular, the measured index at 405 nm is 1.670, and a new polymer is available with an index at that wavelength of approximately 1.68. Therefore, at the average emission wavelength of 400 nm for the scintillator, the index of the plastic is slightly larger than that of the crystals. If necessary, the polymer can be diluted with a low index copolymer to match the crystals. (When polymerized within the new polymer, the crystals are invisible in white light.) Since the emission spectrum is only 90 nm wide, differences in dispersion between crystal and plastic should not introduce harmful light scattering problems, at least in thin layers.

Table II shows the various materials available for neutron detection and the energy ranges of applicability.

Table III lists the calculated and observed parameters for several materials.

Table IV lists the calculated efficiencies for four materials of interest. The effect of replacing natural gadolinium with low cross section yttrium or depleted gadolinium is significant at these energies.

Figure 1 shows the emission spectrum of $Li_6Gd(BO_3)_3(Ce)$ and Li_6 Y $(BO_3)_3(Ce)$ when excited by 340 nm UV light. The emission spectrum is well matched to the response functions of inexpensive PM tubes. The emission spectrum for charged-particle excitation is essentially identical.

Figure 2 is a plot of the pulse-height spectrum from a 1-mm thick single crystal of LiGdB. The peak near channel 380 is due to ^{6}LI capture, and the peak near channel 80 is due to ^{10}B capture. The crystal was grown with B enriched to 95% in B-10.

Figure 3 is a plot of the spectrum for the same material in microcrystalline form incorporated in casting resin.

Figure 4 is a plot of the pulse-height spectrum for a 1-mm thick sheet of GS-20 Li glass scintillator irradiated with thermal neutrons.

Figure 5 is a plot of ground GS-20 incorporated in an index-matching plastic polymer.

APPENDIX

The gamma-background sensitivity of several neutron detector materials was measured at the ISIS facility. The collimated neutron beam inpinged upon a cylinder of Cd, with the various detectors placed approximately 30 cm out of the beam and shielded from scattered neutrons. The relative response of the detectors was calculated from the observed number of background counts in a window centered at the position of the neutron capture peak, of width 2 x FWHM. The listed background sensitivity is the number of background counts per incident neutron per gm of ^{6}Li in the detector.

Table I
SCINTILLATOR COMPARISON
RELATIVE PULSE HEIGHT

Material	^{10}B(n, alpha)	^{6}Li(n,alpha)	Gd(n,gamma)
$Li_6Gd(BO_3)_3$	1.0	1.0	1.0
BC-454 (plastic)	0.09	—	—
GS-20 (glass)	—	0.165	—
GSO (crystal)	—	—	0.52
	PE/neutron*	**PE/neutron**	**PE/MeV**
Li_6 Gd $(BO_3)_3$	1290	6200	2780

*PE = Detected photoelectrons in PM tube.

Table II
DETECTOR OVERVIEW

COLD	10meV	THERMAL	150meV	EPITHERMAL
		^{7}Li Ln (^{10}B)		^{7}Li Ln (^{10}B)
^{3}He		(^{6}Li) Ln ^{11}B		(^{6}Li) Ln ^{11}B
Zn S (^{6}Li)		^{3}He		Zn S (^{6}Li)
		Zn S (^{6}Li)		^{6}Li glass
		^{7}Li (Ln) ^{11}B		

Li Ln B = Li_6 Ln $(B0_3)_3$ (Ce)

Ln = natural Gd, depleted Gd, Y

Table III
MATERIAL CHARACTERISTICS

	^{6}Li-Glass	$Li_6Gd(BO_3)_3$ (Li capture)	$Li_6Gd(BO_3)_3$ (B capture)
Atomic Density (X 10^{22} atoms cm^{-3})	1.72 (Li)	3.30 (Li)	1.65 (B)
Macroscopic Capture Cross Section (cm^{-1}) (at thermal)	16.1	30.9	63.3
Density (gm cm^{-3})	2.5	3.5	3.5
Relative Signal Amplitude for Alpha Particles	1.0	5.8	5.8
Relative Signal Amplitude for Neutron Capture	1.0	6.0	1.3
Neutron Capture, Peak Electron Energy Equivalent (MeV)	1.48	2.22	0.46
Alpha-to-Beta Ratio	0.23	0.30	0.30
Scintillation Decay time	60 ns	200 ns 700 ns (small)	200 ns 700 ns (small)
Index of refraction	1.55	1.66	1.66
Melting Point	1200°c	860°c	860°c

Table IV
DETECTION EFFICIENCY COMPARISON

Neutron Energy	0.25 mm Li YB (B-10 Capture)	0.25 mm Li Gd B (B-10 Capture)	0.25 mm Li Gd B (Li-6 Capture)	BC704 (Li-6 Capture)
0.025eV	80%	63%	43%	29%
0.10eV	56%	52%	30%	13%
0.20eV	44%	43%	23%	11%

Li Gd B with available Gd, depleted in odd isotopes.

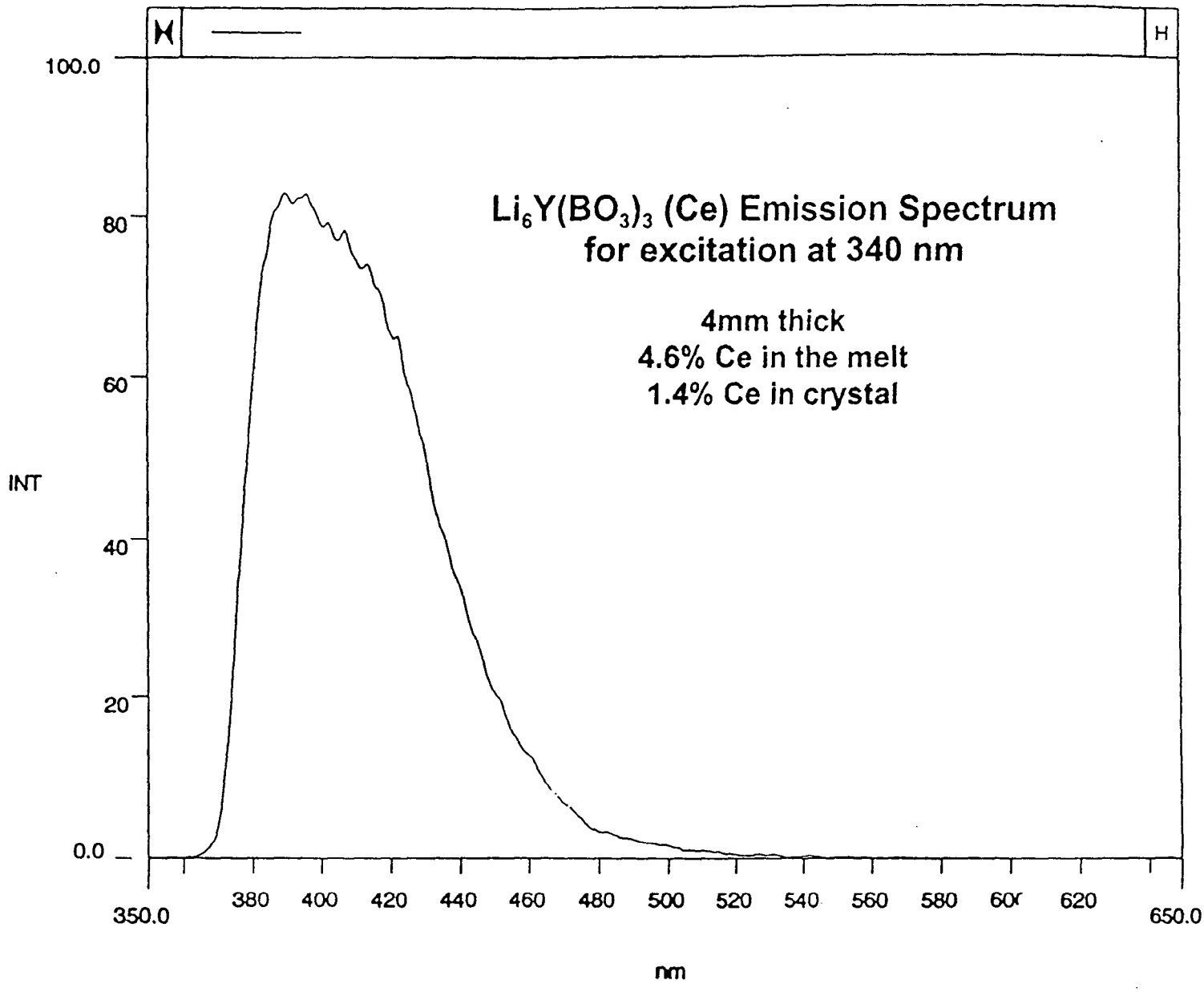
100.0
80
60
40
20
0.0
INT
350.0
380
400
420
440
460
480
500
520
540
560
580
620
650.0
nm
H
$Li_6Y(BO_3)_3$ (Ce) Emission Spectrum
for excitation at 340 nm
4mm thick
4.6% Ce in the melt
1.4% Ce in crystal

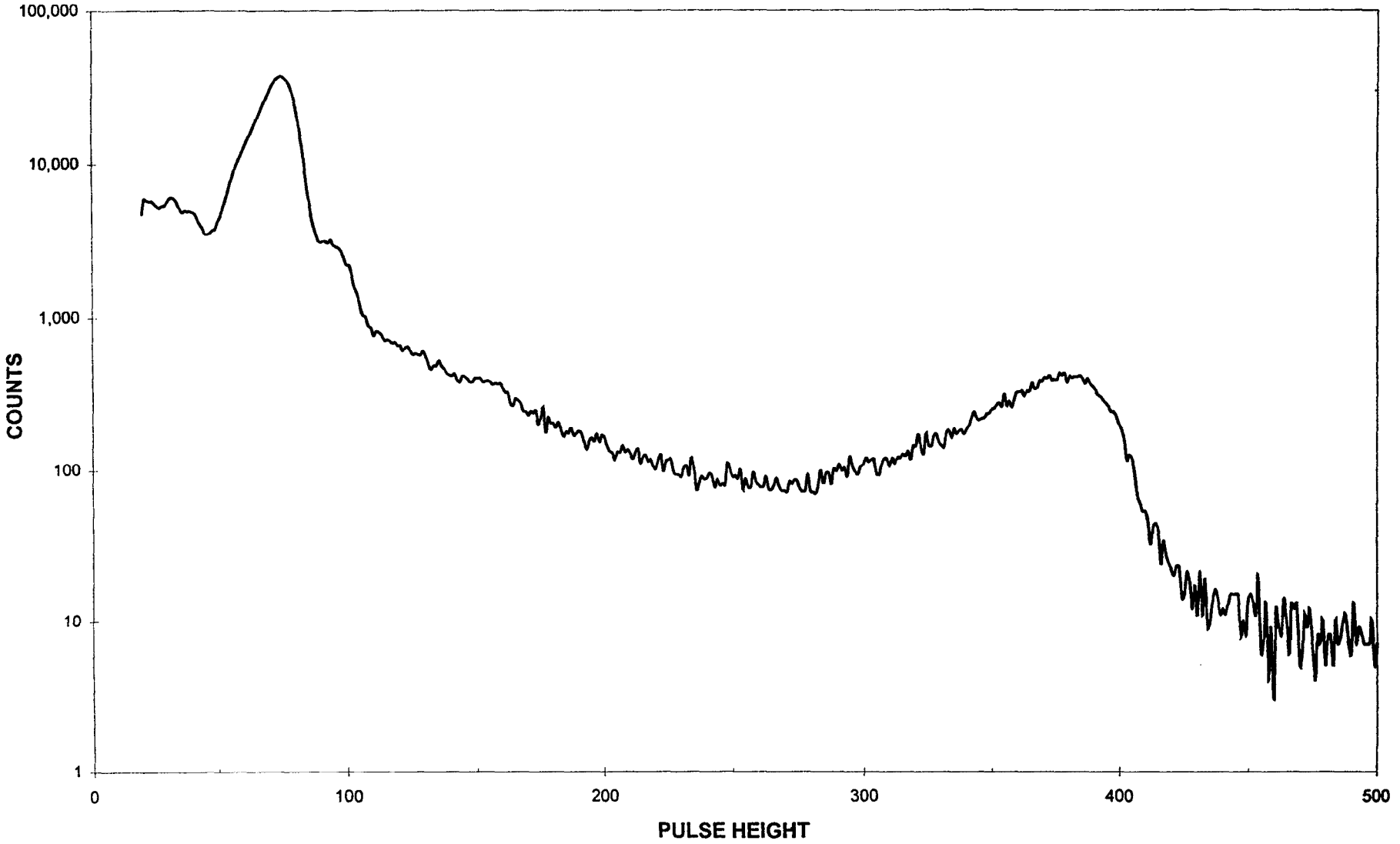
100,000
10,000
1,000
100
10
1
COUNTS
0
100
200
300
400
500
PULSE HEIGHT

FIGURE 2

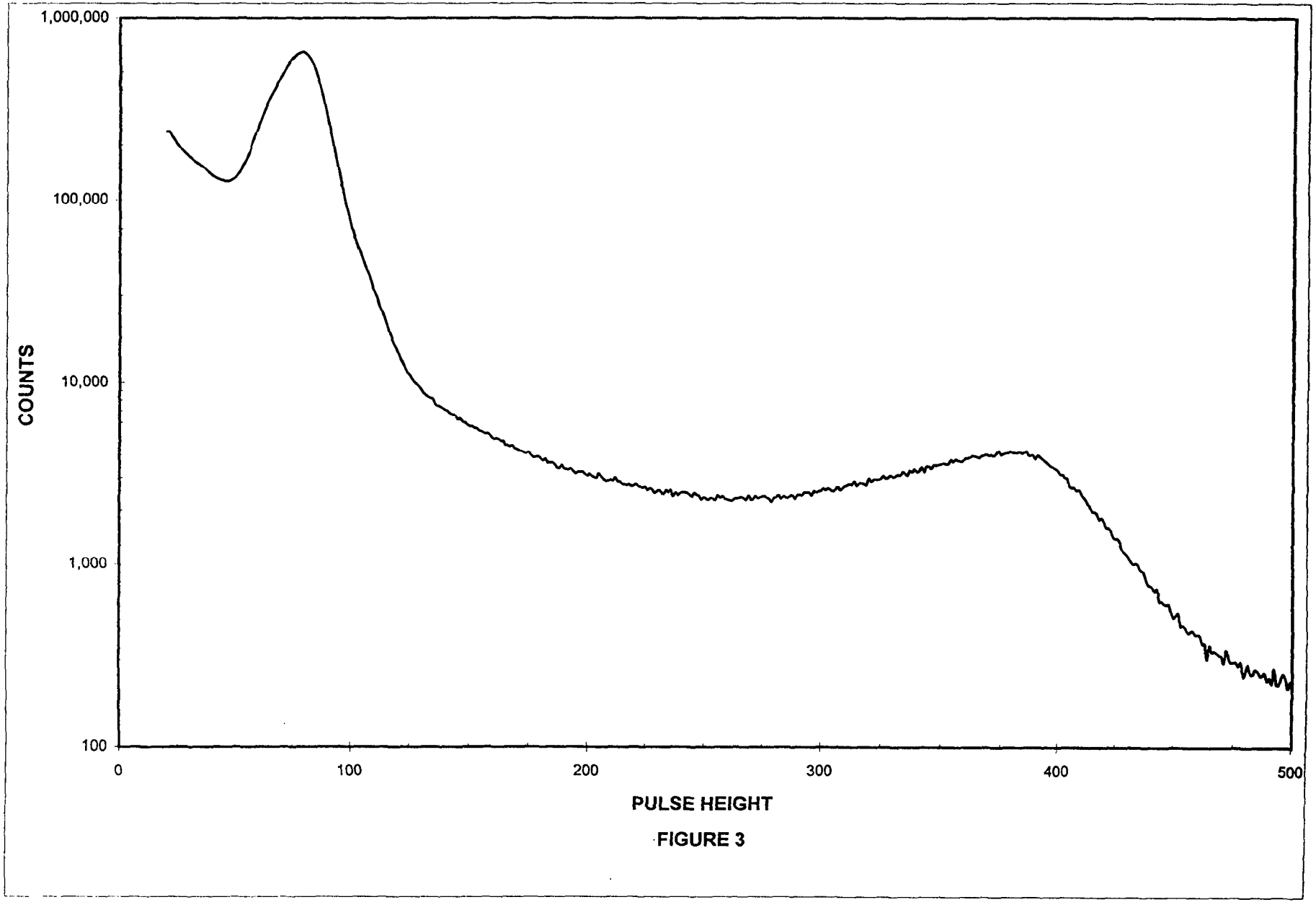
1,000,000
100,000
10,000
1,000
100
COUNTS
0
100
200
300
400
500
PULSE HEIGHT

FIGURE 3

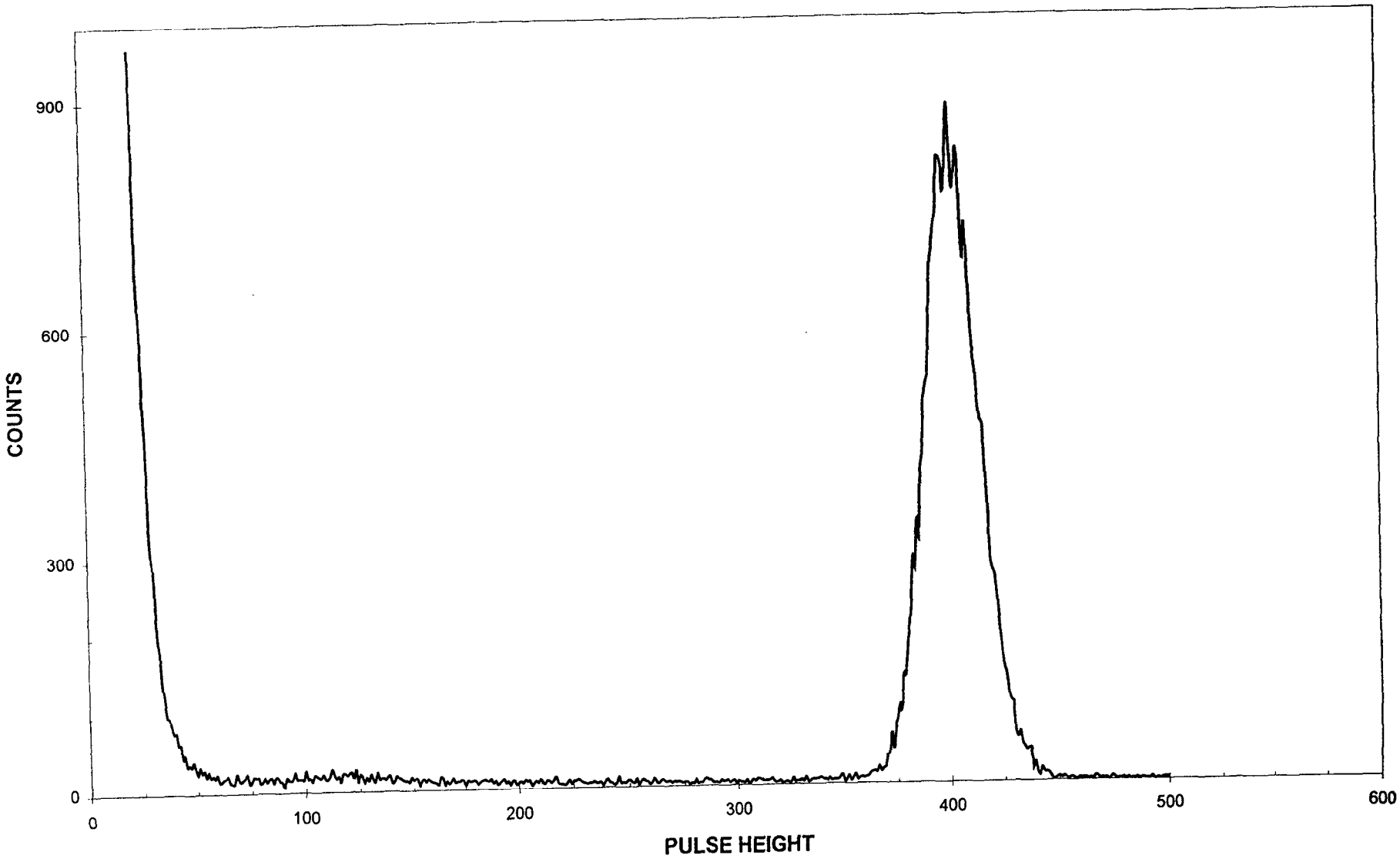

FIGURE 4

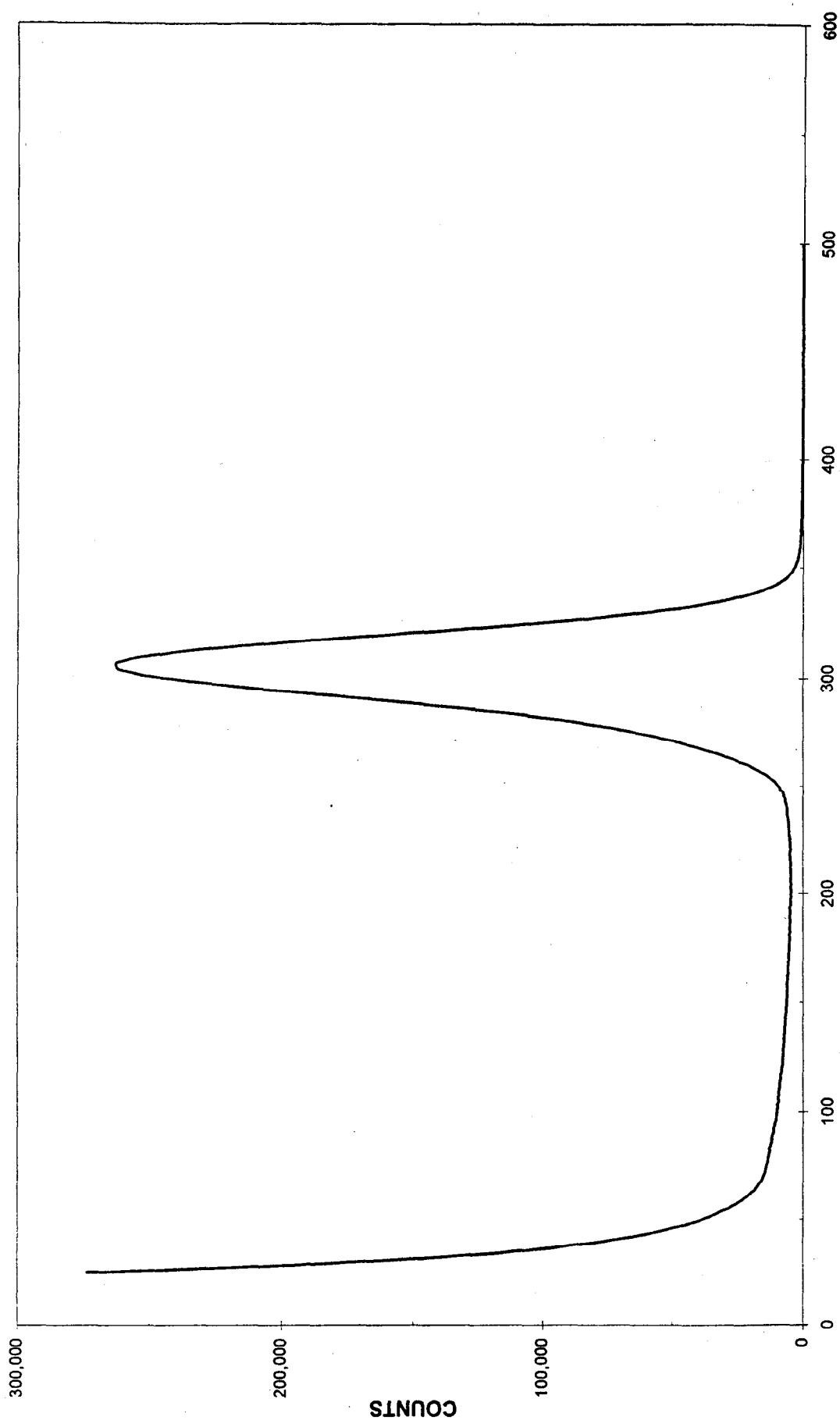
COUNTS
300,000
200,000
100,000
0
0
100
200
300
400
500
600
PULSE HEIGHT

FIGURE 5

Appendix Table I
Relative Detector Background Sensitivity

Material	Thickness $\frac{\text{mg } {}^{6}\text{Li}}{\text{cm}^2}$	$\frac{\text{Background Counts}}{\text{Neutron} \bullet \text{g } {}^{6}\text{Li}}$
GS-20 (glass)	31.4	1.0
GS-20 (glass)	23.5	0.91
GS-20 (glass)	15.7	0.54
GS-20 (glass)	7.9	0.20
LiGd Borate (single crystal)	22.6	0.16
GS-20+Polymer	3.8	0.74